PLOS ONE

RESEARCH ARTICLE

Tetraarsenic hexoxide induces G2/M arrest, apoptosis, and autophagy via PI3K/Akt suppression and p38 MAPK activation in SW620 human colon cancer cells

Arulkumar Nagappan[1], Won Sup Lee[1]*, Jeong Won Yun[1], Jing Nan Lu[1¤], Seong-Hwan Chang[2], Jae-Hoon Jeong[3], Gon Sup Kim[4], Jin-Myung Jung[5], Soon Chan Hong[6]

1 Department of Internal Medicine, Institute of Health Sciences, Gyeongsang National University School of Medicine, 90 Chilam-dong Jinju, Korea, **2** Department of Surgery, Konkuk University School of Medicine, Seoul, Korea, **3** Research Center for Radiotherapy, Korea Institute of Radiological and Medical Sciences, Seoul, Korea, **4** Research Institute of Life Science and College of Veterinary Medicine, Gyeongsang National University, 900 Gajwadong, Jinju, Korea, **5** Department of Neurosurgery, Institute of Health Sciences, Gyeongsang National University School of Medicine, 90 Chilam-dong Jinju, Korea, **6** Department of Surgery, Institute of Health Sciences, Gyeongsang National University School of Medicine, 90 Chilam-dong Jinju, Korea

¤ Current address: The fifth hospital of Shijiazhuang, Shijiazhuang, China
* lwshmo@hanmail.net, lwshmo@gnu.ac.kr

Citation: Nagappan A, Lee WS, Yun JW, Lu JN, Chang S-H, Jeong J-H, et al. (2017) Tetraarsenic hexoxide induces G2/M arrest, apoptosis, and autophagy via PI3K/Akt suppression and p38 MAPK activation in SW620 human colon cancer cells. PLoS ONE 12(3): e0174591. https://doi.org/10.1371/journal.pone.0174591

Editor: Salvatore V. Pizzo, Duke University School of Medicine, UNITED STATES

Received: November 17, 2016

Accepted: March 11, 2017

Published: March 29, 2017

Data Availability Statement: All relevant data are within the paper and its Supporting Information files.

Funding: The present study was supported by a grant from the National Research Foundation of Korea (NRF) funded by the Korea government (MEST) (no. 20120002631), in part by a grant of the National R&D Program for Cancer Control, Ministry for Health, Welfare and Family Affairs, Republic of Korea (0820050).

Abstract

Tetraarsenic hexoxide (As_4O_6) has been used in Korean folk medicines for the treatment of cancer, however its anti-cancer mechanisms remain obscured. Here, this study investigated the anti-cancer effect of As_4O_6 on SW620 human colon cancer cells. As_4O_6 has showed a dose-dependent inhibition of SW620 cells proliferation. As_4O_6 significantly increased the sub-G1 and G2/M phase population, and Annexin V-positive cells in a dose-dependent manner. G2/M arrest was concomitant with augment of p21 and reduction in cyclin B1, cell division cycle 2 (cdc 2) expressions. Nuclear condensation, cleaved nuclei and poly (adenosine diphosphate-ribose) polymerase (PARP) activation were also observed in As_4O_6-treated SW620 cells. As_4O_6 induced depolarization of mitochondrial membrane potential (MMP, $\Delta\Psi m$) but not reactive oxygen species (ROS) generation. Further, As_4O_6 increased death receptor 5 (DR5), not DR4 and suppressed the B-cell lymphoma-2 (Bcl-2) and X-linked inhibitor of apoptosis protein (XIAP) family proteins. As_4O_6 increased the formation of AVOs (lysosomes and autophagolysosomes) and promoted the conversion of microtubule-associated protein 1A/1B-light chain 3 (LC3)-I to LC3-II in a dose- and time- dependent manner. Interestingly, a specific phosphoinositide 3-kinase (PI3K)/Akt inhibitor (LY294002) augmented the As_4O_6 induced cell death; whereas p38 mitogen-activated protein kinases (p38 MAPK) inhibitor (SB203580) abrogated the cell death. Thus, the present study provides the first evidence that As_4O_6 induced G2/M arrest, apoptosis and autophagic cell death through PI3K/Akt and p38 MAPK pathways alteration in SW620 cells.

Competing interests: The authors have declared that no competing interests exist.

Introduction

Colorectal cancer (CRC) is the third most common type of cancer and the second leading cause of cancer related death in the world [1]. CRC represents a major public health problem and the incidence of CRC has recently been increasing especially in Korea [2]. Most of the colorectal cancers belong to the adenocarcinomas accounting with approximately 95% of cases. The 5 years survival rates are very poor for patients, those diagnosed at their advanced stages. Recently survival rates of CRC patients have improved with the help of advanced modality in the cancer research. Despite treatments for CRC including surgery, radiation therapy and/or chemotherapy are generally available, its application still very limited and cause severe side effects [3]. Thus, there is necessity for development of novel therapeutic potential for the CRC prevention and therapy.

Induction of the cell cycle arrest and programmed cell death are the important strategies in the cancer prevention and therapeutics. Apoptosis (type I programmed cell death) and autophagy (type II programmed cell death) are the two major modes of programmed cell death playing an imperative roles in cancer chemoprevention [4, 5]. Both apoptosis and autophagy plays essential roles in development, tissue homeostasis and disease in organisms. The ample evidences indicate that therapeutic agents act through the mechanisms involving cell cycle alteration, apoptosis and autophagic cell death on wide variety of human cancer cell [6–8]. In addition, therapeutic agents may also affects the cell death and survival of multi-signaling pathways within the cells, including Tumor necrosis factor (TNF), TNF-related apoptosis-inducing ligand (TRAIL), PI3K/Akt and mitogen-activated protein kinases (MAPKs) mediated pathways etc [9–12]. Therefore, investigating the mechanism of cell death in colon cancer cells would be helpful to develop novel strategy to treat the colon cancer.

Arsenical compounds have been used in Traditional Chinese Medicines (TCM) for thousands of years to treat a variety of medical diseases, including cancer [13]. Thus, arsenicals have drawn much attention in recent years since its successful clinical application as arsenic trioxide (As_2O_3, ATO) for treating acute promyelocytic leukemia (APL) [14]. In addition, As_2O_3 exhibited the anti-cancer properties in various cell lines such as gallbladder carcinoma cells [15], mouse embryonic fibroblasts [16], human cervical cancer cells [17], leukemic cell lines [18, 19] and malignant glioma cells [20]. Similarly, tetraarsenic oxide (As_4O_6, TAO) is a natural substance obtained from Sinsuk, and has been used in traditional medicine in Korea for the management of many type of solid cancer. Besides, different from As_2O_3, As_4O_6 was widely used in Korea in the late 1980' and 1990' because it showed some anecdotal cases showing dramatic effects without noticeable side effects. However, only limited studies have exhibited the anti-cancer effect of As_4O_6 in human cancer cells, suggesting that the mechanisms of As_4O_6-induced cell death are also different from As_2O_3 [21, 22]. Our previous study has also demonstrated that As_4O_6 has anticancer properties through suppression of NF-κB activity in SW620 cells [23]. However, the anticancer effect and the detailed mechanisms of As_4O_6 and its cell regulatory action remain obscured in colorectal cancer.

Here, we have investigated the anti-cancer effect and their molecular mechanism of the As_4O_6-induced cell death in SW620 human colorectal cancer cells. Our results provide the novel mechanism which includes As4O6 induced G2/M arrest, apoptosis and autophagic cell death by suppression of PI3K/Akt mechanism and further activating p38 MAPK pathways in SW620 cells.

Materials and methods

Cells and reagents

SW620 human colon cancer cells from the American type culture collection (Rockville, MD, USA) were cultured in RPMI 1640 medium (Invitrogen Corp, Carlsbad, CA, USA)

supplemented with 10% (v/v) fetal bovine serum (FBS) (GIBCO BRL, Grand Island, NY, USA), 1 mM L-glutamine, 100 U/mL penicillin, and 100 μg/mL streptomycin at 37˚C in a humidified atmosphere of 95% air and 5% CO_2. As_4O_6 was obtained from Chonjisan institute (Seoul, Korea). Antibodies against procaspase 3, poly (ADP-ribose) polymerase (PARP), β-catenin, DR4, DR5, Bax, Bcl-2, Bid, cyclin B1, XIAP, p21, AKT 1/2/3 (H-136), phospho-Akt (Ser473), ERK, phospho-ERK (E-4), p53 and Beclin 1 were purchased from Santa Cruz Biotechnology (Santa Cruz, CA, USA). Antibodies against LC3, and Beclin-1, were purchased from PharMingen (San Diego, CA, U.S.A.). Antibodies against phospho-Akt (Thr 308), procaspase 8, procaspase 9, phospho-p38 MAPK, cdc2, JNK, and phospho-JNK were purchased from Cell signaling Technology, Inc. (Beverly, MA, USA). Antibody against β-actin was purchased from Sigma (Beverly, MA). Peroxidase-labeled donkey anti-rabbit and sheep anti-mouse immunoglobulin, and an enhanced chemiluminescence (ECL) kit were purchased from Amersham (Arlington Heights, IL, USA). All other chemicals not specifically cited here were purchased from Sigma Chemical Co. (St. Louis, MO, USA).

Cell viability assay

The effect of As_4O_6 on cell proliferation of SW620 cells was assessed by MTT (3-(4,5-Dimethylthiazol-2-yl)-2,5-Diphenyltetrazolium Bromide) assay [24]. The SW620 cells were seeded onto 12-well plates (10×10^4), and then treated with As_4O_6 (0, 0.1, 0.5, 1, 2 and 5 μM) for 24 h and 48 h. MTT powder (0.5 mg/ml) was subsequently added to each well and incubated for 3 h. And then, 500 μl of DMSO was added to dissolve the crystals. The absorption values were determined at 570 nm with an ELISA plate reader. Cell morphology was photographed under light microscopy (magnification, x200).

Nuclear staining

Morphological changes in cell nuclei was determined by 4,6-diamidino-2-phenylindole (DAPI) staining as described previously [25]. The SW620 cells were seeded in 24-well plates at a density of 5×10^4 cells/mL per well and incubated for 24 h. Cells were treated with As_4O_6 at 0, 0.1, 0.5, 1, 2 and 5 μM concentrations, washed the harvested cells with phosphate-buffered saline (PBS) and fixed with 3.7% paraformaldehyde in PBS for 10 min at room temperature. After washed with PBS, the cells were stained with 2.5 μg/ml DAPI solution for 10 min at room temperature. After the cells were washed two times again with PBS, the images of stained nuclei were captured by the NIS-Element AR 3.2 imaging software (Nikon Instruments Inc, NY, USA).

Propidium iodide (PI) staining for cell cycle analysis and Annexin V-FITC/PI staining for apoptosis by flow cytometry assay

The SW620 cells were plated at a concentration of 2×10^5 cells/well in six-well plates and incubated with As_4O_6 at 0, 0.1, 0.5, 1, 2 and 5 μM for 24 h. The cells were collected, washed with cold PBS, and then centrifuged. For PI staining, the pellet was fixed in 75% (v/v) ethanol for 1 h at 4˚C. The cells were washed once with PBS and re-suspended in cold PI solution (50 μg/ml) containing RNase A (0.1 mg/ml) in PBS (pH 7.4) for 30 min in the dark. Annexin V double staining was performed according to manufactures instructions. Briefly, 5 μL of the annexin V conjugate was added to each 100 μL of cell suspension for 15 min, and then 400 μL of annexin V-binding buffer was added and mixed gently, keeping the samples on ice. Flow cytometry analyses were performed with beckman coulter cytomics FC 500 (Becton Dickinson, San Jose, CA).

Measurement of MMP (ΔΨm) and ROS generation

The SW620 cells were seeded onto 6-well plates (2×10^5) and then treated with As_4O_6 at 0, 0.1, 0.5, 1, 2 and 5 μM concentrations for 24 h and MMP (ΔΨm) in living cells was measured by flow cytometry with the lipophilic cationic probe JC-1, a ratiometric, dual-emission fluorescent dye [26] There are two excitation wavelengths, 527 nm (green) for the monomer form and 590 nm (red) for the J-aggregate form. The cells were harvested and re-suspended in 500 μL of PBS, incubated with 10 μM JC-1 for 20 min at 37˚C. Quantitation of green fluorescent signals reflects the amount of damaged mitochondria. For ROS measurement [27], the cells were incubated with 10 μM 2′,7′-dichlorofluorescein diacetate (DCFDA) at 37˚C for 30 min. The cells were then washed with ice-cold PBS and harvested. Fluorescence was determined with beckman coulter cytomics FC 500 (Becton Dickinson, San Jose, CA, USA).

Western blot analysis

The SW620 cells were seeded onto 6-well plates (2×10^5) and then treated with As_4O_6 at 0, 0.1, 0.5, 1, 2 and 5 μM concentrations for 24 h. Total cell lysates were obtained after treated with RIPA buffer (25 mM Tris (pH 7.6), 150 mM NaCl, 1% NP-40, 1% sodium deoxycholate and 0.1% SDS) and protease inhibitors. The protein concentration was determined by Bradford protein assay (Biorad lab, Ricmond, CA, USA). Approximately, 30 μg of lysate was resolved on 10–12% SDS-PAGE, electrotransferred to polyvinylidene difluoride membranes (Millipore, Bedford, MA, USA), and then incubated with specific primary antibodies (1:1000) at 4˚C overnight followed by secondary antibody (1:1000) conjugated to peroxidase. Blots were developed with an ECL detection system.

Inhibitors assay

To identify the role of PI3K/Akt and MAPKs on As4O6-induced apoptosis and autophagy in SW620 cells, where 10 μM SB203580 (Specific p38 MAPK Inhibitor), 10 μM LY294002 (a specific PI3K/Akt inhibitor) were pretreated 1hr before As_4O_6 (1 μM) treatment. After incubation with As_4O_6 for 48 h, further experiments were conducted.

Analysis of Acidic Vesicular Organelles (AVOs) with acridine orange staining

The SW620 cells were incubated with As_4O_6 at 0, 0.1, 0.5, 1, 2 and 5 μM concentrations for 24 h. Then, the cells were stained with acridine orange dye. Green (510–530 nm) and red (650 nm) fluorescence emission from cells illuminated with blue (488 nm) excitation light was measured by flow cytometry analyses with beckman coulter cytomics FC 500 (Becton Dickinson, San Jose, CA, USA).

Statistics

Data was expressed as means ± standard deviation (SD). Significant differences were determined using the one-way ANOVA with post-test Neuman-Keuls for more than two group comparison and Student's *t* test for two group comparison. Statistical significance was defined as $p<0.05$. All experiments were performed in triplicate.

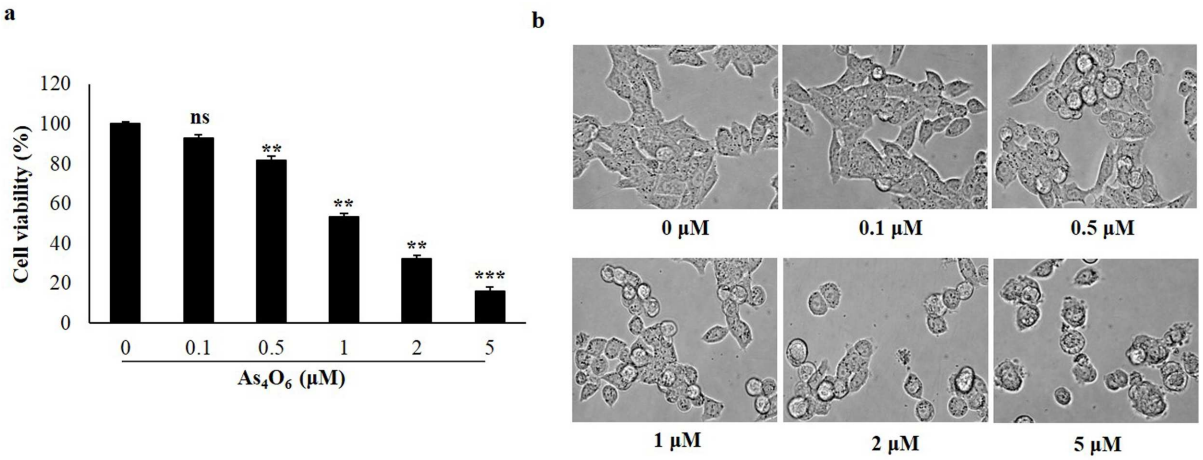

Fig 1. As_4O_6 inhibited proliferation of SW620 cells. The cells were seeded at the density of $5x10^4$ cells per ml. (a) The inhibition of cell proliferation was measured by MTT assay. The cells were treated with As_4O_6 at 0, 0.1, 0.5, 1, 2 and 5 μM concentrations for 24 h. The antiproliferation of As_4O_6 is shown in a dose-dependent manner. (b) Cellular morphology was observed under light microscope (Magnification, X 400). The data are shown as means ± SD of three independent experiments. 'ns' represents not significant; '*' represents significance (**p<0.01 and *** p<0.001between the treated and the untreated control group).

https://doi.org/10.1371/journal.pone.0174591.g001

Results

Anti-proliferative effect of As_4O_6 on SW620 human colon cancer cells

To investigate the anti- proliferative activity of As_4O_6, observation was done by 3-(4,5-dimethythiazol- 2-yl)- 2,5-diphenyl tetrazolium bromide (MTT) assay, known to be a colorimetric assay used to determine the reduction of MTT by mitochondrial succinate dehydrogenase in the living cells. In order to assess the cell viability, SW620 cells were incubated with As_4O_6 at 0, 0.1, 0.5, 1, 2 and 5 μM concentrations for 24 h and 48 h. The results showed that As_4O_6 significantly inhibited the proliferation of SW620 cells in a dose-and time-dependent manner, where the 50% inhibitory concentration (IC50) was estimated approximately at 1μM (Fig 1A & S1 Fig). However, no significant differences were found in cell viability between 24 h and 48 h of As_4O_6 treatment. Hence, our further experiments were conducted at 24 h treatment with As_4O_6. In order to observe the changes in cellular morphology of As_4O_6-treated SW620 cells, examination has been done under light microscopy. The results indicated that the cells with morphological changes such as round shape, cell shrinkage and decrease in cell numbers were observed at 1 μM, 2 μM and 5 μM concentrations of As_4O_6 treatment (Fig 1B). These findings suggest that As_4O_6 could inhibit the proliferation of SW620 human colon cancer cells.

As_4O_6 induced apoptosis with G2/M cell cycle arrest in SW620 cells

In order to determine, whether the decrease in cell viability of SW620 cells was caused by the induction of apoptotic cell death, flow cytometry was performed. The cell cycle distribution in SW620 cells was examined after treatment with As_4O_6 at 0, 0.1, 0.5, 1, 2 and 5 μM for 24 h. The cells with G2/M phase and sub-G1 DNA content were significantly increased in a dose-dependent manner (Fig 2A & 2B). To investigate the further mechanisms responsible for G2/M arrest induced by As_4O_6 in SW620 cells, immuno-blotting was performed. The p21, cyclin B1 and cdc2 proteins are crucial in G2/M phase transition process. A complex of cyclin B1 and CDK1 proteins are controlling the G2/M phase, and complex is regulated by cdc25c [28]. The immune-blotting results revealed that As_4O_6 increased p21 expression and decreased the expression levels of cyclinB1 and cdc2 proteins in a dose-dependent manner at 24 h treatment

period (Fig 2C). These data suggest that As_4O_6 induce G2/M arrest by regulation of p21, cyclin B1 and cdc2 proteins in SW620 cells.

Further, to investigate the apoptotic cell death in As_4O_6 treated SW620 cells, Annexin V-FITC/PI apoptosis assay was perfomed to confirm that above finding is derived from apoptosis. The obtained results showed that the apoptotic cells were significantly increased in a dose-dependent manner (Fig 3A). As shown in Fig 3B, DAPI staining revealed that normal nuclei of untreated cells had an intact round morphology, whereas the apoptotic nuclei of cells treated with As_4O_6 showed chromatin condensation and fragmented nuclei (Fig 3B). These findings suggest that As_4O_6 treatment could induce apoptosis in SW620 cells.

As_4O_6 induced the depolarization of mitochondrial membrane potential (MMP, ΔΨm), caspase activation and subsequent cleavage of PARP

In apoptosis induction process, mitochondrial depolarization is important mechanism during mitochondrial mediated pathway[29]. Hence, observation has been taken to measure the

a

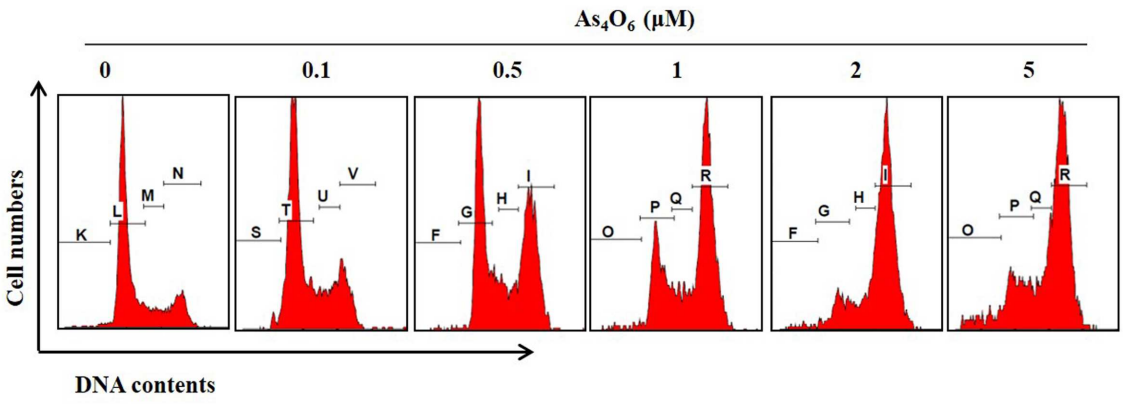

b

As_4O_6 (μM)	Sub-G1	G1	S	G2/M
0	3.57	65.02	11.52	19.29
0.1	3.79	54.44	16.35	21.71
0.5	4.04	40.12	15.57	42.20
1	6.17	23.26	12.82	56.82
2	5.86	13.39	13.26	69.46
5	9.85	20.91	15.97	50.99

c

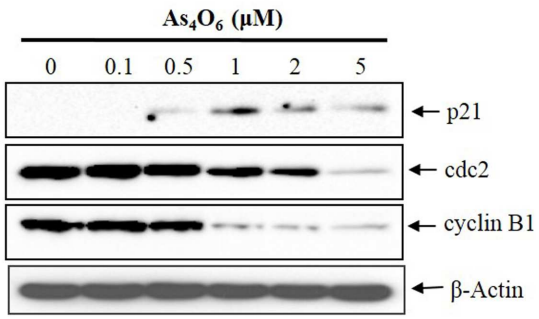

Fig 2. As_4O_6 induced G2/M cell cycle arrest of SW620 cells. The cells were seeded at the density of $5x10^4$ cells per ml. (a) To quantify the cell cycle phase distribution, the cells were treated with As_4O_6 at 0, 0.1, 0.5, 1, 2 and 5 μM concentrations for 24 h and stained with PI followed by flow cytometry was performed. (b) Quantitative data represents G2/M arrest was induced by As_4O_6 on SW620 cells in a dose dependent manner. (c) The cells were treated with As_4O_6 at 0, 0.1, 0.5, 1, 2 and 5 μM concentrations for 24 h. Total cell lysates were resolved by SDS-polyacrylamide gels and transferred onto nitrocellulose membranes. The membranes were probed with the p21, cyclin B1, cdc2 antibodies. To confirm equal loading, the blot was stripped of the bound antibody and reprobed with the anti β-actin antibody. The proteins were visualized using an ECL detection system. The data are shown of three independent experiments.

https://doi.org/10.1371/journal.pone.0174591.g002

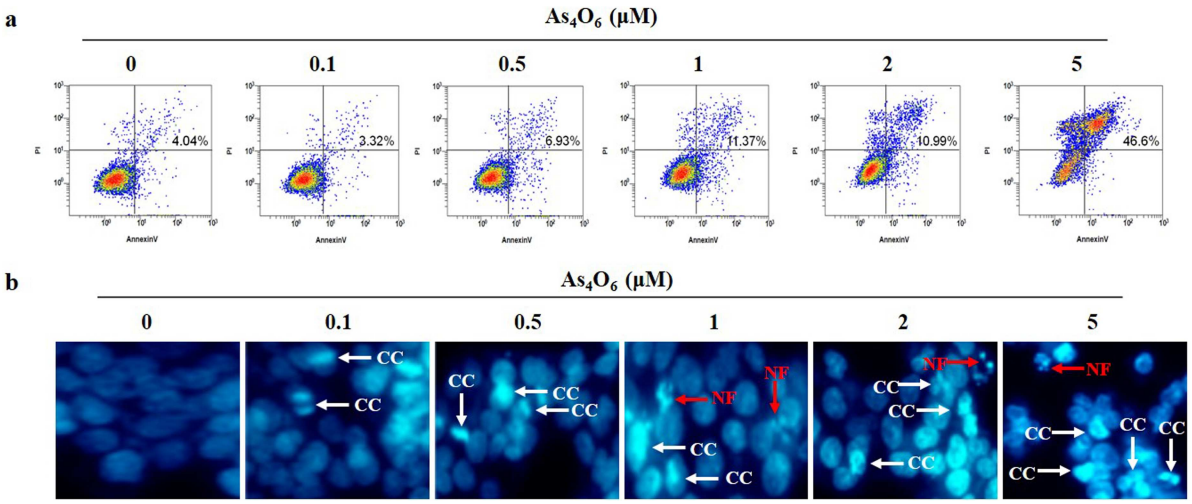

Fig 3. As_4O_6-induced apoptosis in SW620 cells. The cells were seeded at the density of $5x10^4$ cells per ml. (a) To quantify the extent of As_4O_6-induced apoptosis, the cells were treated with As_4O_6 at 0, 0.1, 0.5, 1, 2 and 5 μM concentrations for 24 h and Annexin V was analyzed by flow cytometry. (b) After fixation, the cells were stained with DAPI solution to observe apoptotic body. Stained nuclei were then observed under fluorescent microscope using a blue filter (Magnification, X 400). CC represents chromatin condensation; NF represents nuclear fragmentation. The data are shown of three independent experiments.

https://doi.org/10.1371/journal.pone.0174591.g003

changes in mitochondrial membrane potential (ΔΨm) by flow cytometry with JC-1 staining after As_4O_6 treatment for 24 h. The results indicated that the depolarization of MMP was induced at 2 and 5 μM of As_4O_6 in SW620 cells (Fig 4A). Hence, the finding suggests that As_4O_6 -induced apoptosis was associated with mitochondrial pathway in As_4O_6 -induced apoptotic cell death. Moreover, ROS generation is also an important mechanism for mitochondria-related apoptosis [29, 30]. Further process was carried out to determine the ROS generation in As_4O_6-treated SW620 cells by flow cytometry, where H_2O_2 used as a positive control to induce ROS production. The results showed that As_4O_6 did not induce ROS production in SW620 cells (S2 Fig), suggesting that As_4O_6 induced apoptosis was not due to ROS generation.

To find out whether As_4O_6 induced caspase-dependent cell death in SW620 cells, further assessment was done to observe the effects of As_4O_6 on caspases protein and their substrate (PARP). Expectedly, western blot analysis revealed that As_4O_6 activated the caspase-3, caspase-8, and caspase-9 whereas the cleavages of PARP were clearly observed in a dose- dependent manner (Fig 4B). It has been reported that cleavages of PARP considered as hallmark of apoptosis [31]. These findings revealed that As_4O_6 could induce caspase-dependent apoptosis in SW620 cells.

Effects of As_4O_6 on death receptors (DR4 and DR5), Bcl-2 family members and X-linked inhibitor of apoptosis (XIAP)

To investigate whether extrinsic pathways are involved in As_4O_6 induced apoptotic cell death, observation was done to examine the expression of TRAIL receptors (DR4, DR5). Western blot analysis revealed that DR5 was up-regulated at 2 and 5 μM of As_4O_6 treatment, but not DR4 (Fig 4C). Further, it has been observed that, As_4O_6 also suppressed the expression of Bcl-2, and XIAP (anti-apoptotic proteins) whereas an expression of Bax (pro-apoptotic protein) was increased in a dose-dependent manner (Fig 4C). However, As_4O_6 did not influence the expression of Bad and Bid.Taken together, these findings suggest that As_4O_6 induces apoptosis

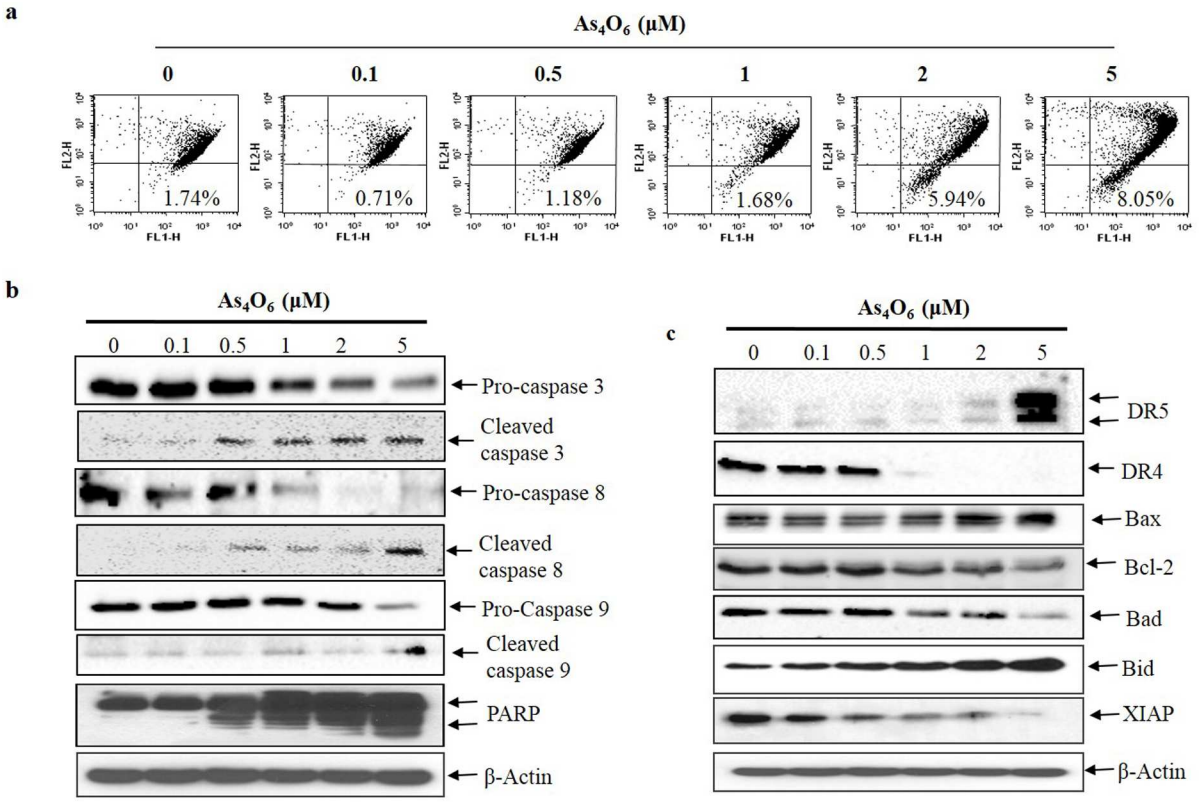

Fig 4. As_4O_6 induces MMP (ΔΨm) depolarization, activates of caspases and cleavage of PARP, and DR5 as well as regulation of Bcl-2, IAP family. The cells were incubated at 0, 0.1, 0.5, 1, 2 and 5 μM concentrations of As_4O_6 for 24 h. (a) The cells were stained with JC-1 and incubated at 37˚C for 30 min. The mean JC-1 fluorescence intensity was assessed by a flow cytometer. As_4O_6 induced depolarization of MMP (ΔΨm) at 2 and 5 μM concentrations. (b) Total cell lysates were resolved by SDS-polyacrylamide gels and transferred onto nitrocellulose membranes. The membranes were probed with the anti-caspase-3, anti-caspase-8, anti-caspase-9 and anti-PARP antibodies. (c) The membranes were probed with the antibodies against DR4, DR5, Bcl-2 and IAP family members. To confirm equal loading, the blot was stripped of the bound antibody and reprobed with the anti β-actin antibody. The proteins were visualized using an ECL detection system. The data are shown of three independent experiments.

https://doi.org/10.1371/journal.pone.0174591.g004

by up-regulating DR5 which is involved in extrinsic pathway, and that apoptosis is augmented by modulating Bcl-2 and IAP family members which is involved in intrinsic pathway.

As_4O_6 induced autophagic cell death in SW620 cells

To investigate the autophagic cell death, examination was performed to observe whether As_4O_6 treatment induced autophagy in SW620 cells. Further, autophagy markers microtubule-associated protein1 light chain3 (LC3) and Beclin 1 were analyzed by western blot analysis. During autophagy, a cytosolic form of LC3 (LC3-I) is conjugated to phosphatidylethanolamine to form membrane-bound form of LC3 (LC3-II). In this study, two variants of LC3 were detected in western blot, where in the ratio of LC3-II/LC3-I has shown to increase in a dose- and time -dependent manner (Fig 5A; meanwhile, no changes were observed in Beclin 1 in SW620 cells. Interestingly, PARP-1 activation is essential in the autophagy process during the response to chemotherapeutic agent [32]. Hence it has already been observed in Figs 4B & 5A, that As_4O_6 induced cleavages of PARP in a dose- and time-dependent manner. In addition, autophagy is characterized by increased formation of AVOs (lysosomes and autophagolysosomes). Hence, formation of AVOs in As_4O_6-treated SW620 cells were analyzed by flow cytometry with

acridine orange (AO) dye, supporting the obtained result that As4O6-induced the accumulation of AVOs in a dose-dependent manner (S3 Fig). Taken together, the results suggest that As_4O_6 induced Beclin-1 independent autophagy by promoting the conversion of LC3-I to LC3-II followed by PARP activation & cleavage in SW620 cells.

As_4O_6 suppressed Akt, and JNK and activated p38, and ERK in SW620 cells

To elucidate the mechanisms for As_4O_6–induced cancer cell death, Western blots analysis has been experimented on Akt and MAPKs phosphorylation to determine whether As_4O_6 regulates the phosphorylation or dephosphorylation of Akt and MAPKs, which is closely related to cancer cell survival and death [33]. Western blot analysis revealed that As_4O_6 remarkably dephosphorylated Akt and JNK in a dose- and time dependent manner (Fig 5B and S4 Fig). Meanwhile, phosphorylation of p-38 MAPK and ERK were significantly increased in a dose- and time dependent manner (Fig 5B and S4 Fig). Moreover, inhibitors of JNK (SP600125) and ERK (PD98059) could not influence the apoptosis induced by As_4O_6 in SW620 cells (S4 Fig). Hence, we hypothesized that As_4O_6 may induce cell death by suppression of PI3K/Akt and activation of p38 MAPK in SW620 cells.

Involvement of PI3K/AKT pathway in As_4O_6 induced cell death in SW620 cells

Evidence suggests that PI3K/Akt pathway plays pivotal role in regulating cell cycle, apoptosis and autophagy [34, 35]. To assess whether As_4O_6 induced cell death was mediated by PI3K/

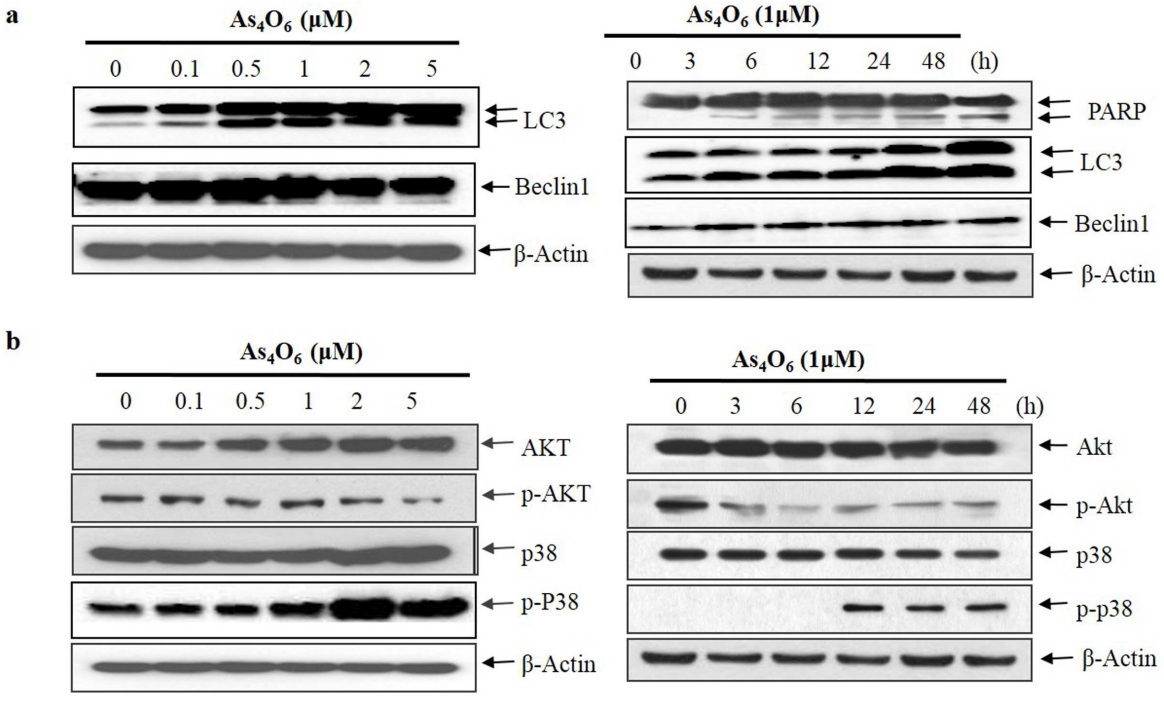

Fig 5. Modulation of autophagy markers, Akt, and p38 MAPK expressions in As_4O_6-treated SW620 cells. The cells were treated with As_4O_6 at 0, 0.1, 0.5, 1, 2 and 5 μM concentrations for the indicated time intervals. For western blot analysis of (a) Beclin1, LC3, PARP and (b) Akt, and p38 MAPK, equal amounts of cell lysate (30 μg) were resolved by SDS-polyacrylamide gels and transferred onto nitrocellulose membranes. To confirm equal loading, the blot was stripped of the bound antibody and reprobed with the anti ß-actin antibody. The results are from at least three independent experiments that showed similar patterns.

https://doi.org/10.1371/journal.pone.0174591.g005

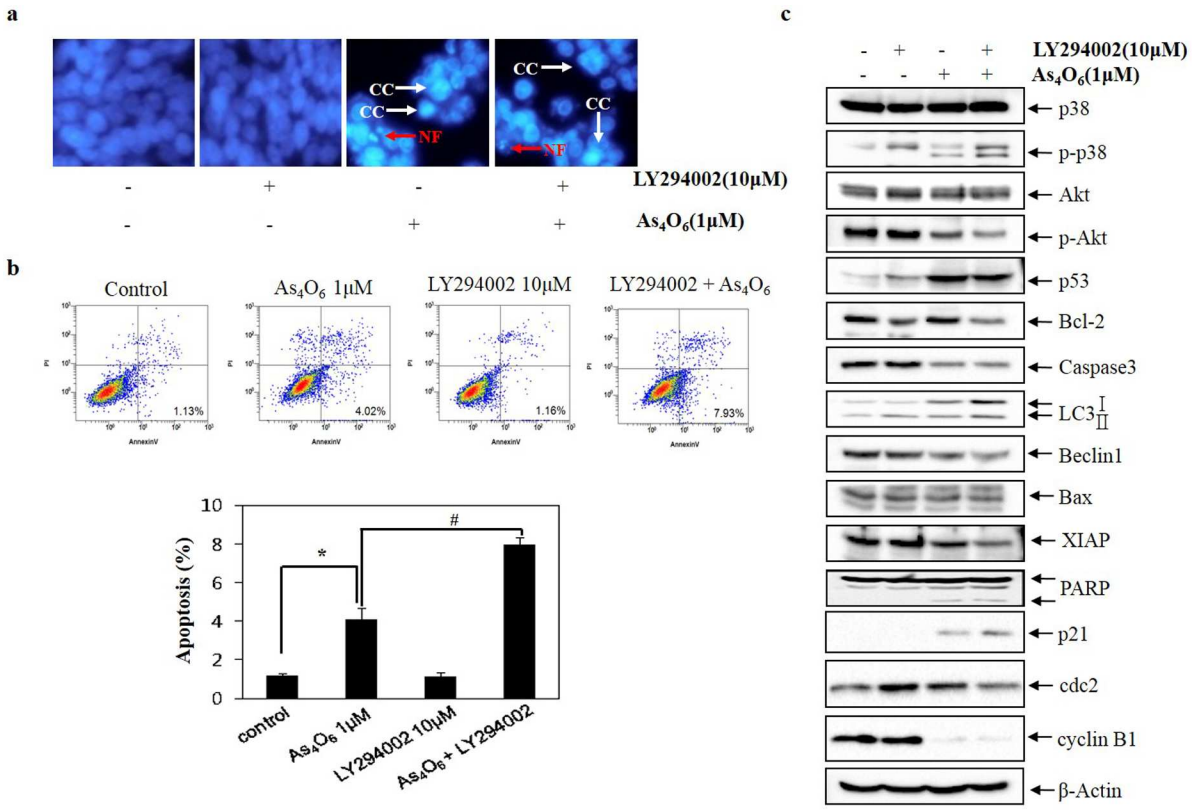

Fig 6. Role of Akt in As4O6 induced cell death in SW620 cells. The cells were treated with LY294002 (10 μM) 30 minute before treatment with As_4O_6 (1 μM) for 48 h. (a) To confirm apoptosis, the cells were stained with DAPI solution after fixation. Stained nuclei were then observed under fluorescent microscope using a blue filter (Magnification, X 400). CC represents chromatin condensation; NF represents nuclear fragmentation. (b) Apoptosis was assessed by Annexin V/PI flow cytometry assay. (c) Equal amounts of cell lysate (30 μg) were resolved by SDS-polyacrylamide gels and transferred onto nitrocellulose membranes. To confirm equal loading, the blot was stripped of the bound antibody and reprobed with the anti ß-actin antibody. The data are shown as mean ± SD of three independent experiments. * $p<0.05$ between the treated and the untreated control group.; # $p<0.05$ compared between the combination treatment group (LY294002 and As_4O_6) and As_4O_6 alone treatment group.

https://doi.org/10.1371/journal.pone.0174591.g006

Akt, analysis has been done to observe the cells using flow cytometry after As_4O_6 treatment, where the changes in nuclear morphology of As_4O_6-treated cells was done by DAPI staining. The DAPI staining revealed that LY294002 (specific PI3K/Akt inhibitor) increased condensed and fragmented nuclei in the As_4O_6-treated SW620 cells (Fig 6A). In addition, it has been found that LY294002 augmented the As_4O_6-induced cell death (Fig 6B). To confirm this finding at the molecular level, and to determine whether this cell death is associated with PI3K/Akt pathway, western blotting was undertaken. It revealed that the addition of LY294002 to As_4O_6 treatment augmented the effects of As_4O_6 on cell cycle regulatory proteins: the expression of p21 and cyclin B1, on apoptosis: the expression of XIAP, Bcl-2, PARP cleavage, and on autophagy: LC3 conversion (Fig 6C). Altogether, these findings suggested that PI3K/Akt pathway is involved in As_4O_6 induced G2/M arrest and cell death.

Involvement of p38 MAPK in As_4O_6 induced cell death in SW620 cells

MAPKs signaling pathways are also involved in survival, proliferation, cell cycle, apoptosis and autophagy [36, 37]. ERKs, JNKs and the p38 MAPKs are three major groups of MAPKs. As previously mentioned JNK and ERK could not influence the apoptosis induced by As_4O_6 in SW620 cells, the possible role of p38 MAPK in the As_4O_6-induced cell death was examined.

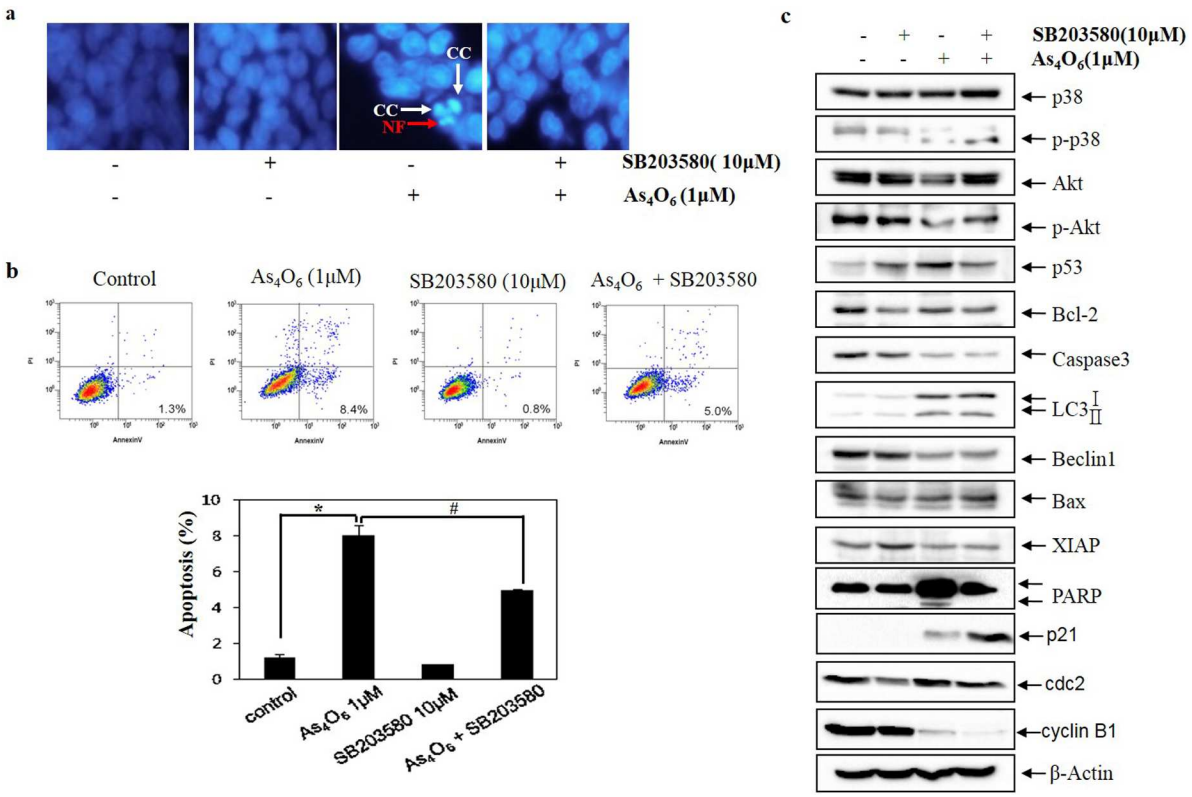

Fig 7. The role of p38 MAPK in As_4O_6-induced cell death in SW620 cells. SW620 cells were treated with SB203580 (10 μM) before As_4O_6 (1 μM) for 48 h. (a) To confirm apoptosis, the cells were stained with DAPI solution after fixation. Stained nuclei were then observed under fluorescent microscope using a blue filter (Magnification, X 400). CC represents chromatin condensation; NF represents nuclear fragmentation. (b) Apoptosis was assessed by Annexin V/PI flow cytometry assay. (c) The cells were lysed and equal amount of the lysate was separated by SDS-polyacrylamide gels, and then transferred to nitrocellulose membranes. The membranes were probed with the indicated antibodies, and detected by an ECL detection system. To confirm equal loading, the blot was stripped of the bound antibody and reprobed with the anti ß-actin antibody. The data are shown as mean ± SD of three independent experiments. * $p<0.05$between the As_4O_6-treated and the untreated control group; # $p<0.05$ compared between the combination treatment group (SB203580 and As_4O_6) and As_4O_6 alone treatment group.

https://doi.org/10.1371/journal.pone.0174591.g007

Hence, the cells were analyzed using flow cytometry after As_4O_6 treatment, where the changes in nuclear morphology of As_4O_6-treated cells were done by DAPI staining. The DAPI staining revealed that p38 MAPK Inhibitor (SB203580) reduced the frequency of condensed and fragmented nuclei in the As_4O_6-treated SW620 cells (Fig 7A). Further, obtained result revealed that p38 MAPK Inhibitor reduced the As_4O_6-induced cell death (Fig 7B). To confirm this finding at the molecular level, and to determine whether the Beclin-1-induction is associated with p38 MAPK Inhibitor, western blot examination was carried out for the molecules involved in As_4O_6-induced apoptosis and autophagy. It revealed that SB203580 suppressed As_4O_6-induced G2/M arrest by restoring the expression of cdc2, and abrogated As_4O_6-induced apoptosis and autophagy by blocking the activation PARP and restored the expression of XIAP, and p-Akt (Fig 7C).These findings suggested that the activation of p38 MAPK is also involved in As_4O_6 induced G2/M arrest and cell death of SW620 cells.

Discussion

In our previous study, was demonstrated that anticancer activity of As_4O_6 through suppression of NF-κB activity in SW620 cells [23]. The present study was designed to investigate the

further mechanisms for the anti-cancer effects of As_4O_6, especially on the cell death. The results revealed that As_4O_6 induced G2/M arrest, apoptosis and autophagy in SW620 cells. The anti-cancer effects of As_4O_6 was associated with PI3K/Akt and p38 MAPK-mediated pathways. To our knowledge, this is the first study report showing multiple anti-cancer mechanisms of As_4O_6 in SW620 cells; As_4O_6 induced G2/M arrest, apoptosis and autophagy via PI3K/Akt and p38 MAPK-mediated pathways, which is unique from other studies.

Firstly, As_4O_6 exhibited strong anti-proliferative activity on SW620 cells, and induced accumulations of sub-G1 population (apoptotic cell population) and G2/M phase populations. The G2/M phase progression is controlled by cyclin B1 and CDK1 complex, which is regulated even by cdc25c. Here, in this study obtained immuno-blotting results indicated that As_4O_6 significantly increased p21 and decreased cyclin B1, and cdc 2 proteins expression in SW620 cells. Previous studies have also demonstrated that the anti-proliferative effects of arsenic compounds were linked to a G2/M phase cell cycle arrest in various cancer cells[38, 39]. Hence these results indicate that As_4O_6 induced G2/M arrest might be associated with down-regulation of cyclin B1 and CDK1 complex and up-regulation of p21.

In addition, there is an association with accumulation of G2/M phase population and apoptosis [40]. Hence, As_4O_6-induced apoptosis was confirmed by FITC-Annexin V and PI double staining, nuclear condensation, cleaved nuclei and PARP activation. These findings suggest that As_4O_6 could induce apoptosis in SW620 cells. To elucidate the molecular mechanism of anti-cancer effect of As_4O_6, immune-blotting was performed. Apoptosis can be executed through either extrinsic pathway and/or intrinsic pathway [41]. In this study, As_4O_6 significantly activated the caspase -3, -8 and -9 and induced PARP cleavage has been observed in SW620 cells (Fig 4A). The pattern of cleavages in PARP (89 kDa), can be distinguished from necrosis or other type of cell death, which indicated that As_4O_6-induced cell death is caspase-dependent apoptosis [42]. The pathway is involved in mitochondrial outer membrane permeabilization cofers a critical event in apoptosis [43]. The up-regulated of DR5 and activation of caspase 8 by As_4O_6 suggests that As_4O_6 induced apoptosis through extrinsic pathway. Apart from death receptors, mitochondrial membrane potential is also important in inducing apoptosis. Further, our results showed that As_4O_6 induced depolarization of mitochondrial membrane potential (MMP), but not ROS generation. Taken together, As_4O_6-induced apoptosis in SW620 cells might be contributed through extrinsic pathway via DR5 up-regulation as well as mitochondrial mediated intrinsic pathways. This apoptosis was augmented by the modulation of Bcl-2 and IAP family members, which support our results that As_4O_6 induced apoptosis might attributed through multiple mechanisms.

The findings of this study also suggested that the As_4O_6 induced autophagy or type II programmed cell death could be another mechanism for As_4O_6 induced cell death. In this study, two variants of LC3 were detected in western blot, where in the ratio of LC3-II/LC3-I increased in a dose- and time-dependent manner (Fig 5A). Although this finding appears similar to As_2O_3 in colon cancer cell death [19, 44] it is different from As_2O_3 induced cell deaths, which is Beclin-1-independent autophagic cell death. However, it may not be a unique finding of As_4O_6-induced autophagy because it recently has been reported that arsenic trioxide also induces a Beclin-1-independent autophagic cell death in ovarian cancer cells [45]. In addition PARP-1 activation is also an essential process in the autophagy during the response to chemotherapeutic agent [32]. Our results also showed similar patterns that the conversion of LC3-I to LC3-II and PARP activation & cleavage. These results revealed that autophagy might contribute to the anti-cancer activity of As_4O_6.

Regarding up-stream signaling, it was demonstrated that As_4O_6-induced apoptosis is closely related to activation of p38 MAPK and suppression of Akt activities. MAPKs composed of three major groups (ERKs, JNKs and the p38 MAPKs) that are mainly involved in cell

survival, proliferation and apoptosis [36, 37]. Hence, we examined the phosphorylation status of MAPKs by western blotting to elucidate the molecular mechanisms that are involved in As_4O_6-induced apoptosis in SW620 cells. The present study showed that As_4O_6 dephosphorylated JNK, and phosphorylated p38 and ERK, but JNK and ERK signaling pathways was not involved in As_4O_6-induced cell death. The cell death was blocked by p38 MAPK inhibitor; suggesting p38 MAPK was associated with As_4O_6-induced cell death (Fig 6). Different from previous study, we found that the activation of p38 MAPK was associated with As_4O_6-induced cell death of SW620 cells. In general, the activation of p38 MAPK is associated cell cycle arrest and apoptosis at early time of treatments. Furthermore, our study demonstrated that As_4O_6 dephosphorylated Akt, which has been reported in regulating cell proliferation and apoptosis, and that a specific PI3K/Akt inhibitor augmented As_4O_6-induced cell death in SW620 cells (Fig 7). These findings suggest that PI3KAKT pathway also involved in As_4O_6-induced cell death of SW620 cells. Taken together, our findings support that p38 MAPK and PI3K/Akt pathways might be attributed to the As_4O_6-induced cell death of SW620 cells.

The limitation of this study is that some scientists believe that there is no functional difference between As_4O_6 and As_2O_3 in dissolved status. In addition, in human body, 3+ form changes into 5+ form and even these two are changing from one into another and they also get methylated in human body. Furthermore, this oxidation of As3+ into As5+ was variable depending on growth media or expose to light conditions. Here, we did not clearly determine the oxidation status of As_4O_6. Here, we just focus on the mechanisms of the anti-cancer effects of As_4O_6 to explain the case showing some clinical improvement; this study helps to understand the clinical cases showing long-term stable disease with central necrosis. It could be explained by p38 MAPK-associated dormant status with apoptosis and autophagy that was related to Akt/PI3K.

Conclusions

In the present study, we have demonstrated that the anti-cancer mechanism for As_4O_6-induced G2/M arrest, apoptosis and autophagy in SW620 cells. Furthermore, As_4O_6 suppressed the PI3K/Akt and activated the p38 MAPK. These activities might play a critical role in As_4O_6-induced cell death of SW620 cells. Lastly, this study provides the evidence that As_4O_6 has an anti-cancer effects; it might be useful for the understanding the clinical cases showing long-term stable disease with central necrosis.

Supporting information

S1 Fig. As_4O_6 cells time-dependently inhibited proliferation of SW620 cells. The cells were seeded at the density of $5x10^4$ cells per ml. The inhibition of cell proliferation was measured by MTT assay. The cells were treated with As_4O_6 at 0, 0.1, 0.5, 1, 2 and 5 μM concentrations for 24 h and 48 h. The anti-proliferation of As_4O_6 is shown in a dose- and time- dependent manner. The data are shown as means ± SD of three independent experiments. 'ns' represents not significant; '*' represents significance ($^{**}p<0.01$ and $^{***}p<0.001$between the treated and the untreated control group).
(TIF)

S2 Fig. As_4O_6 did not induce ROS generation in SW620 cells. For the assessment of ROS level, the cells were incubated with 10 μM DCF-DA for 30 min after As_4O_6 (2 μM) treatment. H_2O_2 (2Mm) was used as positive control. The fluorescence intensity was assessed by a flow cytometer.
(TIF)

S3 Fig. Effect of As_4O_6 on the autophagy in SW620 cells. The cells were treated with As_4O_6 at 0, 0.1, 0.5, 1, 2 and 5 μM concentrations for 24 h. After incubation, the cells were stained

with 5 μg/mL acridine orange for 17 min and collected in phenol red-free growth medium. Green (510–530 nm) and red (650 nm) fluorescence emission illuminated with blue (488 nm) excitation light was measured with a flow cytometer. As_4O_6 induced dose-dependent AVO formation in SW620 cells.
(TIF)

S4 Fig. Role of ERK and JNK in As_4O_6 induced cell death in SW620 cells. The cells were treated with ERK inhibitor, PD98059 (20 μM) and JNK inhibitor, SP600125 (10 μM) 30 minute before treatment with As_4O_6 (1 μM) for 48 h. (a) For western blot analysis, equal amounts of cell lysate (30 μg) were resolved by SDS-polyacrylamide gels and transferred onto nitrocellulose membranes. To confirm equal loading, the blot was stripped of the bound antibody and reprobed with the anti ß-actin antibody. The data are shown as mean ± SD of three independent experiments. 'ns' represents not significant; '*' represents significance (**$p<0.01$ between the As_4O_6 treated and the untreated control group.
(TIF)

Acknowledgments

The present study was supported by a grant from the National Research Foundation of Korea (NRF) funded by the Korea government (MEST) (no. 20120002631), in part by a grant of the National R&D Program for Cancer Control, Ministry for Health, Welfare and Family Affairs, Republic of Korea (0820050).

Author Contributions

Conceptualization: AN WSL.

Data curation: AN JWY.

Formal analysis: AN WSL SCH.

Funding acquisition: WSL GSK JMJ.

Investigation: AN JNL.

Methodology: AN WSL JWY SCH.

Project administration: WSL.

Resources: WSL JMJ JWY JNL S-HC J-HJ GSK.

Software: AN JWY.

Supervision: WSL.

Validation: AN WSL.

Visualization: AN WSL JNL.

Writing – original draft: AN WSL.

Writing – review & editing: AN WSL GSK.

References

1. Siegel RL, Miller KD, Jemal A. Cancer statistics, 2015. CA Cancer J Clin. 2015; 65(1):5–29. Epub 2015/01/07. https://doi.org/10.3322/caac.21254 PMID: 25559415

2. Jung KW, Won YJ, Oh CM, Kong HJ, Cho H, Lee DH, et al. Prediction of cancer incidence and mortality in Korea, 2015. Cancer Res Treat. 2015; 47(2):142–8. Epub 2015/03/18.; PubMed Central PMCID: PMC4398104. https://doi.org/10.4143/crt.2015.066 PMID: 25779360
3. Van Cutsem E, Cervantes A, Nordlinger B, Arnold D. Metastatic colorectal cancer: ESMO Clinical Practice Guidelines for diagnosis, treatment and follow-up. Ann Oncol. 2014; 25 Suppl 3:iii1–9. Epub 2014/09/06.
4. Nikoletopoulou V, Markaki M, Palikaras K, Tavernarakis N. Crosstalk between apoptosis, necrosis and autophagy. Biochim Biophys Acta. 2013; 1833(12):3448–59. Epub 2013/06/19. https://doi.org/10.1016/j.bbamcr.2013.06.001 PMID: 23770045
5. Thorburn A. Apoptosis and autophagy: regulatory connections between two supposedly different processes. Apoptosis. 2008; 13(1):1–9. Epub 2007/11/09. PubMed Central PMCID: PMC2601595. https://doi.org/10.1007/s10495-007-0154-9 PMID: 17990121
6. Srivastava S, Somasagara RR, Hegde M, Nishana M, Tadi SK, Srivastava M, et al. Quercetin, a Natural Flavonoid Interacts with DNA, Arrests Cell Cycle and Causes Tumor Regression by Activating Mitochondrial Pathway of Apoptosis. Sci Rep. 2016; 6:24049. Epub 2016/04/14. PubMed Central PMCID: PMC4828642. https://doi.org/10.1038/srep24049 PMID: 27068577
7. Wang R, Zhang Q, Peng X, Zhou C, Zhong Y, Chen X, et al. Stellettin B Induces G1 Arrest, Apoptosis and Autophagy in Human Non-small Cell Lung Cancer A549 Cells via Blocking PI3K/Akt/mTOR Pathway. Sci Rep. 2016; 6:27071. Epub 2016/06/01. PubMed Central PMCID: PMC4886687. https://doi.org/10.1038/srep27071 PMID: 27243769
8. Jeong JW, Lee WS, Go SI, Nagappan A, Baek JY, Lee JD, et al. Pachymic Acid Induces Apoptosis of EJ Bladder Cancer Cells by DR5 Up-Regulation, ROS Generation, Modulation of Bcl-2 and IAP Family Members. Phytother Res. 2015; 29(10):1516–24. Epub 2015/07/08. https://doi.org/10.1002/ptr.5402 PMID: 26148472
9. Kim JJ, Lee SB, Park JK, Yoo YD. TNF-alpha-induced ROS production triggering apoptosis is directly linked to Romo1 and Bcl-X(L). Cell Death Differ. 2010; 17(9):1420–34. Epub 2010/03/06. https://doi.org/10.1038/cdd.2010.19 PMID: 20203691
10. Wang S, El-Deiry WS. TRAIL and apoptosis induction by TNF-family death receptors. Oncogene. 2003; 22(53):8628–33. Epub 2003/11/25. https://doi.org/10.1038/sj.onc.1207232 PMID: 14634624
11. Mitsiades CS, Mitsiades N, Koutsilieris M. The Akt pathway: molecular targets for anti-cancer drug development. Curr Cancer Drug Targets. 2004; 4(3):235–56. Epub 2004/05/12. PMID: 15134532
12. Dhillon AS, Hagan S, Rath O, Kolch W. MAP kinase signalling pathways in cancer. Oncogene. 2007; 26(22):3279–90. Epub 2007/05/15. https://doi.org/10.1038/sj.onc.1210421 PMID: 17496922
13. Liu J, Lu Y, Wu Q, Goyer RA, Waalkes MP. Mineral arsenicals in traditional medicines: orpiment, realgar, and arsenolite. J Pharmacol Exp Ther. 2008; 326(2):363–8. Epub 2008/05/09. PubMed Central PMCID: PMC2693900. https://doi.org/10.1124/jpet.108.139543 PMID: 18463319
14. Chen GQ, Zhu J, Shi XG, Ni JH, Zhong HJ, Si GY, et al. In vitro studies on cellular and molecular mechanisms of arsenic trioxide (As2O3) in the treatment of acute promyelocytic leukemia: As2O3 induces NB4 cell apoptosis with downregulation of Bcl-2 expression and modulation of PML-RAR alpha/PML proteins. Blood. 1996; 88(3):1052–61. Epub 1996/08/01. PMID: 8704214
15. Ai Z, Lu W, Qin X. Arsenic trioxide induces gallbladder carcinoma cell apoptosis via downregulation of Bcl-2. Biochem Biophys Res Commun. 2006; 348(3):1075–81. Epub 2006/08/15. https://doi.org/10.1016/j.bbrc.2006.07.181 PMID: 16904648
16. Nutt LK, Gogvadze V, Uthaisang W, Mirnikjoo B, McConkey DJ, Orrenius S. Indirect effects of Bax and Bak initiate the mitochondrial alterations that lead to cytochrome c release during arsenic trioxide-induced apoptosis. Cancer Biol Ther. 2005; 4(4):459–67. Epub 2005/04/23. PMID: 15846091
17. Kang YH, Yi MJ, Kim MJ, Park MT, Bae S, Kang CM, et al. Caspase-independent cell death by arsenic trioxide in human cervical cancer cells: reactive oxygen species-mediated poly(ADP-ribose) polymerase-1 activation signals apoptosis-inducing factor release from mitochondria. Cancer Res. 2004; 64(24):8960–7. Epub 2004/12/18. https://doi.org/10.1158/0008-5472.CAN-04-1830 PMID: 15604259
18. Yang YP, Liang ZQ, Gao B, Jia YL, Qin ZH. Dynamic effects of autophagy on arsenic trioxide-induced death of human leukemia cell line HL60 cells. Acta Pharmacol Sin. 2008; 29(1):123–34. Epub 2007/12/27. https://doi.org/10.1111/j.1745-7254.2008.00732.x PMID: 18158874
19. Goussetis DJ, Altman JK, Glaser H, McNeer JL, Tallman MS, Platanias LC. Autophagy is a critical mechanism for the induction of the antileukemic effects of arsenic trioxide. J Biol Chem. 2010; 285(39):29989–97. Epub 2010/07/27. PubMed Central PMCID: PMC2943259. https://doi.org/10.1074/jbc.M109.090530 PMID: 20656687
20. Kanzawa T, Kondo Y, Ito H, Kondo S, Germano I. Induction of autophagic cell death in malignant glioma cells by arsenic trioxide. Cancer Res. 2003; 63(9):2103–8. Epub 2003/05/03. PMID: 12727826

21. Chang HS, Bae SM, Kim YW, Kwak SY, Min HJ, Bae IJ, et al. Comparison of diarsenic oxide and tetraarsenic oxide on anticancer effects: relation to the apoptosis molecular pathway. Int J Oncol. 2007; 30 (5):1129–35. Epub 2007/03/29. PMID: 17390014

22. Han MH, Lee WS, Lu JN, Yun JW, Kim G, Jung JM, et al. Tetraarsenic Hexoxide Induces Beclin-1-Induced Autophagic Cell Death as well as Caspase-Dependent Apoptosis in U937 Human Leukemic Cells. Evid Based Complement Alternat Med. 2012; 2012:201414. Epub 2011/09/14. PubMed Central PMCID: PMC3170805. https://doi.org/10.1155/2012/201414 PMID: 21912568

23. Lee WS, Yun JW, Nagappan A, Park HS, Lu JN, Kim HJ, et al. Tetraarsenic hexoxide demonstrates anticancer activity at least in part through suppression of NF-kappaB activity in SW620 human colon cancer cells. Oncol Rep. 2015; 33(6):2940–6. Epub 2015/04/08. https://doi.org/10.3892/or.2015.3890 PMID: 25845556

24. Freimoser FM, Jakob CA, Aebi M, Tuor U. The MTT [3-(4,5-dimethylthiazol-2-yl)-2,5-diphenyltetrazolium bromide] assay is a fast and reliable method for colorimetric determination of fungal cell densities. Appl Environ Microbiol. 1999; 65(8):3727–9. Epub 1999/07/31. PubMed Central PMCID: PMC91559. PMID: 10427074

25. De Castro LF, Zacharias M. DAPI binding to the DNA minor groove: a continuum solvent analysis. J Mol Recognit. 2002; 15(4):209–20. Epub 2002/10/17. https://doi.org/10.1002/jmr.581 PMID: 12382239

26. Chiruvella KK, Kari V, Choudhary B, Nambiar M, Ghanta RG, Raghavan SC. Methyl angolensate, a natural tetranortriterpenoid induces intrinsic apoptotic pathway in leukemic cells. FEBS Lett. 2008; 582 (29):4066–76. Epub 2008/11/22. https://doi.org/10.1016/j.febslet.2008.11.001 PMID: 19022252

27. Aranda A, Sequedo L, Tolosa L, Quintas G, Burello E, Castell JV, et al. Dichloro-dihydro-fluorescein diacetate (DCFH-DA) assay: a quantitative method for oxidative stress assessment of nanoparticle-treated cells. Toxicol In Vitro. 2013; 27(2):954–63. Epub 2013/01/30. https://doi.org/10.1016/j.tiv.2013.01.016 PMID: 23357416

28. Donzelli M, Draetta GF. Regulating mammalian checkpoints through Cdc25 inactivation. EMBO Rep. 2003; 4(7):671–7. Epub 2003/07/02. PubMed Central PMCID: PMC1326326. https://doi.org/10.1038/sj.embor.embor887 PMID: 12835754

29. Hengartner MO. The biochemistry of apoptosis. Nature. 2000; 407(6805):770–6. Epub 2000/10/26. https://doi.org/10.1038/35037710 PMID: 11048727

30. Miyajima A, Nakashima J, Yoshioka K, Tachibana M, Tazaki H, Murai M. Role of reactive oxygen species in cis-dichlorodiammineplatinum-induced cytotoxicity on bladder cancer cells. Br J Cancer. 1997; 76(2):206–10. Epub 1997/01/01. PubMed Central PMCID: PMC2223948. PMID: 9231920

31. Gobeil S, Boucher CC, Nadeau D, Poirier GG. Characterization of the necrotic cleavage of poly(ADP-ribose) polymerase (PARP-1): implication of lysosomal proteases. Cell Death Differ. 2001; 8(6):588–94. Epub 2001/09/06. https://doi.org/10.1038/sj.cdd.4400851 PMID: 11536009

32. Munoz-Gamez JA, Rodriguez-Vargas JM, Quiles-Perez R, Aguilar-Quesada R, Martin-Oliva D, de Murcia G, et al. PARP-1 is involved in autophagy induced by DNA damage. Autophagy. 2009; 5(1):61–74. Epub 2008/11/13. PMID: 19001878

33. Aksamitiene E, Kiyatkin A, Kholodenko BN. Cross-talk between mitogenic Ras/MAPK and survival PI3K/Akt pathways: a fine balance. Biochem Soc Trans. 2012; 40(1):139–46. Epub 2012/01/21. https://doi.org/10.1042/BST20110609 PMID: 22260680

34. Franke TF, Hornik CP, Segev L, Shostak GA, Sugimoto C. PI3K/Akt and apoptosis: size matters. Oncogene. 2003; 22(56):8983–98. Epub 2003/12/10. https://doi.org/10.1038/sj.onc.1207115 PMID: 14663477

35. Chang F, Lee JT, Navolanic PM, Steelman LS, Shelton JG, Blalock WL, et al. Involvement of PI3K/Akt pathway in cell cycle progression, apoptosis, and neoplastic transformation: a target for cancer chemotherapy. Leukemia. 2003; 17(3):590–603. Epub 2003/03/21. https://doi.org/10.1038/sj.leu.2402824 PMID: 12646949

36. Raman M, Chen W, Cobb MH. Differential regulation and properties of MAPKs. Oncogene. 2007; 26 (22):3100–12. Epub 2007/05/15. https://doi.org/10.1038/sj.onc.1210392 PMID: 17496909

37. Robinson MJ, Cobb MH. Mitogen-activated protein kinase pathways. Curr Opin Cell Biol. 1997; 9 (2):180–6. Epub 1997/04/01. PMID: 9069255

38. Park JW, Choi YJ, Jang MA, Baek SH, Lim JH, Passaniti T, et al. Arsenic trioxide induces G2/M growth arrest and apoptosis after caspase-3 activation and bcl-2 phosphorylation in promonocytic U937 cells. Biochem Biophys Res Commun. 2001; 286(4):726–34. Epub 2001/08/25. https://doi.org/10.1006/bbrc.2001.5416 PMID: 11520058

39. Zhang X, Jia S, Yang S, Yang Y, Yang T. Arsenic trioxide induces G2/M arrest in hepatocellular carcinoma cells by increasing the tumor suppressor PTEN expression. J Cell Biochem. 2012; 113 (11):3528–35. Epub 2012/06/26. https://doi.org/10.1002/jcb.24230 PMID: 22730174

40. Boonstra J, Post JA. Molecular events associated with reactive oxygen species and cell cycle progression in mammalian cells. Gene. 2004; 337:1–13. Epub 2004/07/28. https://doi.org/10.1016/j.gene.2004.04.032 PMID: 15276197

41. Wong WW, Puthalakath H. Bcl-2 family proteins: the sentinels of the mitochondrial apoptosis pathway. IUBMB Life. 2008; 60(6):390–7. Epub 2008/04/22. https://doi.org/10.1002/iub.51 PMID: 18425793

42. Shah GM, Shah RG, Poirier GG. Different cleavage pattern for poly(ADP-ribose) polymerase during necrosis and apoptosis in HL-60 cells. Biochem Biophys Res Commun. 1996; 229(3):838–44. Epub 1996/12/24. https://doi.org/10.1006/bbrc.1996.1889 PMID: 8954981

43. Borutaite V. Mitochondria as decision-makers in cell death. Environ Mol Mutagen. 2010; 51(5):406–16. Epub 2010/03/09. https://doi.org/10.1002/em.20564 PMID: 20209625

44. Qian W, Liu J, Jin J, Ni W, Xu W. Arsenic trioxide induces not only apoptosis but also autophagic cell death in leukemia cell lines via up-regulation of Beclin-1. Leuk Res. 2007; 31(3):329–39. Epub 2006/08/03. https://doi.org/10.1016/j.leukres.2006.06.021 PMID: 16882451

45. Smith DM, Patel S, Raffoul F, Haller E, Mills GB, Nanjundan M. Arsenic trioxide induces a beclin-1-independent autophagic pathway via modulation of SnoN/SkiL expression in ovarian carcinoma cells. Cell Death Differ. 2010; 17(12):1867–81. Epub 2010/05/29. PubMed Central PMCID: PMC2932795. https://doi.org/10.1038/cdd.2010.53 PMID: 20508647